A New Time of Flight System for the FOPI Detector

Ch. Finck[1] for the FOPI Collaboration
Gesellschaft für Schwerionenforschung Planckstr. 1 D-64291 Darmstadt

Abstract

Experimental data measured with the FOPI detector on kaons rapidity distribution and on directed differential flow have shown hints for in-medium effects. RBUU calculations seems to reproduce the trends in the data when including in-medium effects. In order to extend the measurements of the FOPI detector to large transverse momenta (up to 1 GeV/c) and to systems as heavy as Au + Au, an upgrade project has been started, so as to replace the scintillator barrel with a new time of flight system based on gas detector. New timing GRPC have been built, tested and it has been shown that they can fulfill the FOPI-upgrade requirements. Possible solutions are discussed.

1 Introduction

Studies with heavy ion collisions of sub-threshold strangeness production have received special attention since it has been predicted that hadron properties should change in nuclear medium [1]. This could be related to a partial restoration of the chiral symmetry. As a consequence according to calculation including in-medium effects, the K^+ and K_s^0 mass increases while the K^- effective mass drops with density. In addition the K^+ and K_s^0 mesons feel a weak repulsive potential while the K^- mesons feel a strong attractive potential. This is particularly relevant for heavy ions collisions at beam energy close to the energy threshold for the kaon production. Indeed the K^+ and K_s^0 meson yield should be reduced (increasing of the mass), and the yield of K^- meson should strongly be enhanced. On the other hand, due to their potential in the medium, the kaons K^+ and K_s^0 (K^-) are repelled (attracted) from the high density region region, where they are mostly produced. This influences the phase space populations by widening (narrowing) the K^+ and K_s^0 (K^-) transverse momentum and rapidity distributions, which can be evidence by measuring those distributions and flow observables.

[1]e-mail : c.finck@gsi.de
phone : +49 (0)6159 71 2769
fax : +49 (0)6159 71 2989

Signature for in medium effects have already been found in previous data using KaoS or FOPI detector at highest SIS energy [2, 3, 4]. To pursuit this challenging issue, especially for heavier systems, an upgrade of FOPI was decided. Indeed, due mostly of the performance of the presently used time of flight (ToF) barrel in terms of resolution and of granularity, a clear identification of particles is not possible with heavier colliding system. A new ToF barrel based on gas counter will be implemented and will replace the old scintillator barrel for polar angle $\theta > 35^o$. In order to identify kaons with a reasonable signal-to-background ratio and in order to extend their momentum acceptance up to 1 GeV/c a resolution better than 100 ps is needed. The double hit probability should not exceeded 5 % leading to a granularity of 600 in this angular range.

New developments have been achieved in the last years for better particle identification in order to cope with the multi hit environment reached in heavy ion collisions at high energies. Therefore ToF systems are planned to be used for STAR [5] or ALICE [6] experiments. Contrary to LHC (Large Hadron Collider) [7] or RHIC (Relativistic Heavy Ion Collider) [8] energies, kaons at SIS energies (1-2A GeV) are produced in a sub-threshold regime and therefore the production rates in central collisions are low (10^{-2} and 10^{-4} in central Au + Au collisions at 1.5A GeV for K^+ and K^- respectively). This leads to much higher requirement for the FOPI-ToF system in terms of time resolution and in terms of general performances.

Spark detectors (PesToF) with excellent timing properties ($\sigma < 100$ ps) was developed by Y. Pestov over the last 30 years [9]. There have been applications of such counters in experiments as NA49 at CERN [10], which are still in progress. Recently, in the framework of ALICE-TOF, glass RPC has been developed with micro gap (few 100 μm) cells of 3 $\times$ 3 cm^2 [11]. The measured resolution was less than 50 ps with an efficiency over 99 % for charged pion at 7 GeV/c. The simple and cheap construction with glass and metal electrodes operating with non-flammable gases under atmospheric pressure is a very attractive feature of the GRPC, especially for large TOF systems.

In this article, some important results concerning in medium effects obtained with the FOPI detector will be presented. Results obtained in beam tests with PesToF spark counters and GRPC will be presented. Different solutions for the FOPI-ToF system based on the GRPC will be discussed at the end.

2 FOPI Detector

The FOPI detector is a symmetrical azimuthal 4π detector. It consist of two drift chambers: central drift chamber (CDC) and a forward drift chamber (Helitron) operating in a 0.6 T magnetic field provided by a supra-conductive solenoid magnet. A barrel of 180 scintillator strips surrounds the CDC. A plastic scintillator wall covers the angles $1.2^o < \theta_{lab} < 30^o$. More details about the detector configuration could be found in ref. [12].

The charged particle in the CDC are identified by means of the Bethe-Bloch formula where the energy loss is given by the charge deposited onto the wire and the momentum is deduced from the curvature of the particle tracks in the magnetic field. Moreover the mass and charge is also obtained by the velocity measurement in the ToF barrel, taking the momentum information from the CDC sub-detector. Minimum ionizing particles as protons, pions or kaons with higher momenta ($>$ 0.5 GeV/c) can then be identified with better accuracy. Moreover this double determination of the mass leads also to a reduction of the background in the mass spectrum. The neutral particles are identified by reconstructing the invariant mass spectrum of their decaying products. For instance the K_s^0 mesons are identified by reconstructing the invariant mass spectrum of the pair $\pi^-\pi^+$, the branching ratio is of 69 % in the case.

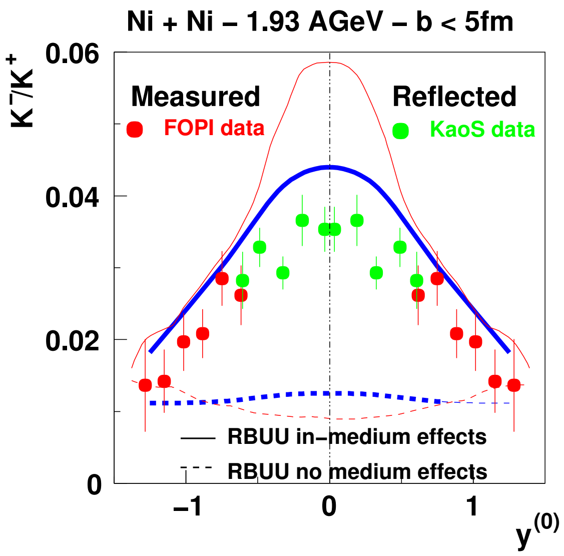

Figure 1: Rapidity distribution of the K^-/K^+ ratio in central collisions for Ni + Ni reaction at 1.93A GeV, measured in the backward hemisphere and reflected for the forward hemisphere. The solid line and dash line are predictions of RBUU calculations with and without including in medium potential, respectively (see text for more details).

3 Motivation for a ToF upgrade

The study of the K^+ and K^- ratio is motivated by several considerations. Since the K^- production yield at SIS energies is small, the limited statistic does not allow a full phase space analysis with high accuracy. Moreover the ratio suffers less from acceptance or inefficiencies of the detector. In addition since in-medium effects act oppositely on K^+ and K^-, their ratio should be a more sensitive observable. Figure 1 shows the rapidity distribution of K^-/K^+ production ratio for Ni + Ni reaction at 1.93A GeV. The data points obtained by the FOPI and the KaoS collaboration with similar centralities are plotted for the same reaction [4, 2]. The data show an enhancement of the ratio in the mid-rapidity region. Since the K^- meson feels an attractive potential, they are preferentially emitted at mid-rapidity where they are mostly produced, whereas the K^+ are slightly repelled from the fireball region. Moreover due to in-medium effects, the K^- yield is enhanced more than the one of K^+. The effect is more pronounced in the mid-rapidity region where the baryon density is the highest. Calculations done with the RBUU code reproduce the trend when including in-medium modification of the kaon mass. The thin lines are predictions taken from ref.[13] and the thick lines are predictions taken from ref. [14]. But there are still discrepancies between models and the data.

The analysis of flow in terms of transverse momentum (p_t) dependence of the first order Fourier coefficient ($v_1 = <p_x/p_t>$ where p_x is the projection onto the reaction plane of the transverse momentum p_t) the so-called differential directed flow (DDF), has been first proposed by the authors of ref.[15]. Figure 2a) shows for the same reaction mentioned above, the DDF for K^+ [3]. Since the data are measured in the backward hemisphere, positive values of v_1 correspond to anti-flow whereas negative values correspond to flow (the DDF for proton is also plotted as reference). Since particles with low transverse momentum are interacting longer with the surrounding medium, the effects are more pronounced at low p_t. The K^+ data clearly show an anti-flow at low p_t. The coulomb interaction also generates a repulsive potential for the K^+. Since an anti-flow is also observed for the neutral kaons K^0_s [16], the effect could not be related to coulomb interaction. Calculations with a BUU model including in-medium effects reproduce nicely the data [14].

Although in the last year a breakthrough was achieved in evidencing in-medium effects and also a big effort was made on the theoretical side to understand the underlying causes, a consistent picture is yet not achieved. Consequently, the FOPI collaboration has decided to extent the space phase especially for kaons, but also for ϕ meson measurements. In particular flow measurements

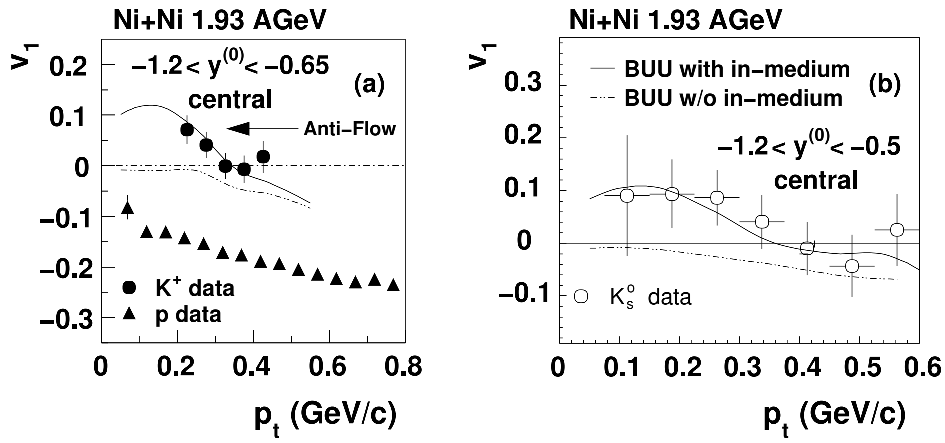

Figure 2: Directed differential flow for K^+ (panel a) and K^0_s (panel b) ratio in central collisions for Ni + Ni reaction at 1.93A GeV, measured in the given rapidity width reported in the figure. The result for proton are plotted as reference. The solid line and dash line are predictions of RBUU calculation with and without including in medium potential, respectively.

of K^- is mandatory, since they feel a strong attractive potential compared to K^+. In addition, higher densities could be achieved with heavier system as Au. In order to be able to measure Au + Au at the highest SIS energy, an upgrade of the FOPI detector has been proposed. Beside the improvement of the performances of the readout capability of data acquisition system, the main part of the project consist of the replacement of the scintillator barrel by a new ToF system.

4 Upgrade of the ToF system

Figure 3 shows the momentum distribution for K^+ (left panel) and for K^- (right panel) for the system Ru + Ru at 1.5A GeV. The solid line is the expected yield given by a RBUU model. The data points represent the expected background in the mass spectrum for the kaon for different ToF resolutions. A full simulation was performed for each momentum bin for the kaon, the mass spectrum was built to determinate the width of the kaon peak. This width is then used to estimate the background in the mass spectrum generate with simulated events containing no kaon.

If kaon momentum should be measurable up to 1 GeV/c, that implies a resolution better than 100 ps, specially for the K^- meson. Moreover the simulation was performed for Ru + Ru system, leading to an under estimation of the background compared to the Au + Au system. If one takes into account the mis-identification due to multi-hits, the granularity of the ToF system must be greater than 600 to

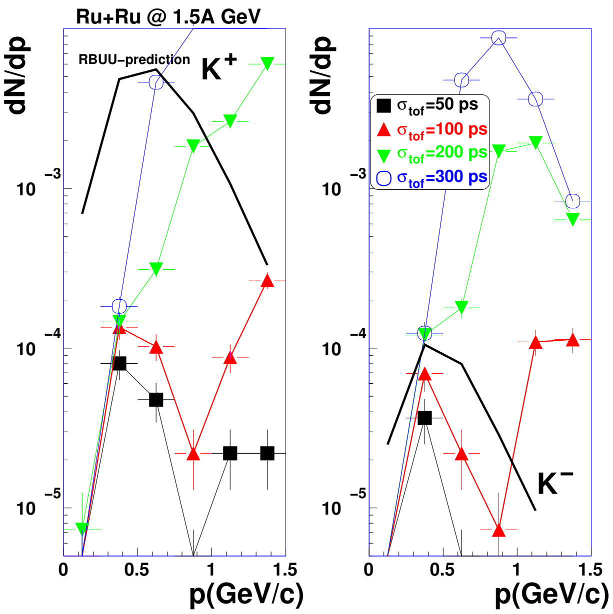

Figure 3: Full simulation of the background in the mass spectra of K^+ and K^- in function of the ToF resolution. The solid lines are yield predictions of RBUU calculations.

keep the double hit probability close to a value of 5 %.

The ToF scintillator in the backward polar angles ($65^o < \theta < 135^o$) has already been replaced by new one meter long strips (material: BC408). Due to the low momenta and multiplicity in this angular range its resolution ($\sigma \sim 130$ ps) and its granularity are sufficient. In the forward angle ($35^o < \theta < 65^o$), where the multiplicity could reach a value of 60 for Au + Au at highest SIS energies, a solution with spark detector PesToF was planned. Later on due to the development of new ToF detectors, a solution with Glass Resistive Plates Chambers (GRPC) was also considered. In the next section, we will report about the beam tests realized with PesToF detectors.

5 PesToF spark counter

The PesToF counter consist of one pressed bulk aluminum plate and a highly resistive glass plate ($5 \times 10^9\ \Omega \cdot cm$). A gap of 100 μm between the two plate is maintained by ball spacers. Both electrodes have an area of 30 $\times$ 4 cm^2 and 2 mm thickness (see fig. 4).

The counter is operated at a pressure of 12 bars sustained by a 1 mm thick aluminum tube containing gas mixtures of the type 20 % C_4H_{10} + 2.5 % C_2H_4 +

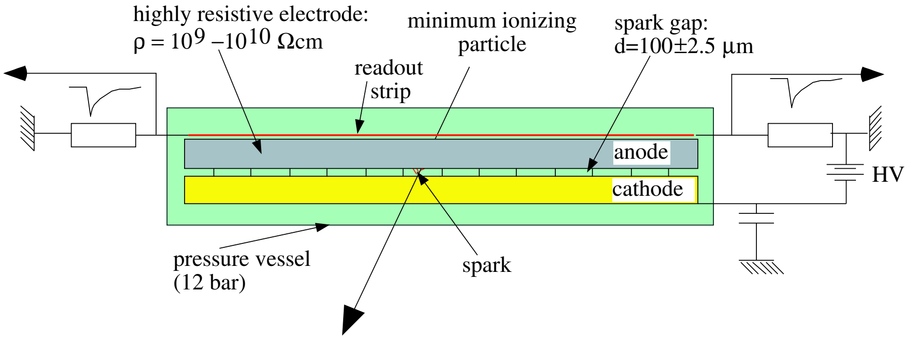

Figure 4: Schematic view of a PesToF detector.

0.5 % C_4H_6 + 77 % of Argon gas. A forced laminar flow through the gap is provided with the help of an extruded plastic profile. A high voltage of about 4.5 kV is applied to the gap. A charged particle traversing the gap producing primary ionization pairs leads, after an avalanche multiplication of 10^8 (corresponding to the Raether condition), to a streamer followed by a spark. At the location of the spark, a large signal is influenced on few of the most closely located metallic strips evaporated onto the back side of the anode glass. More details about the detector working principle could be found in ref. [17]. A 16 fold timing channel readout system is connected to both ends of the 16 strips, while the 16 channel charge measurement is performed at one end of the strips only. For precise time of flight measurements, the counting rate should not exceed about 50 Hz/cm^2 [18]. The time information is derived from the sum of the two time signals measured at both ends of the strip having the highest charge signal.

In view of the specific needs for an application of the Pestov spark counter in the FOPI setup, a 90 cm long detector was produced and tested. Three of the usual glass plates of 30 cm length were used in place of one and an aluminum cathode as well as a multi-strip readout board covering the full length of 90 cm were installed.

A number of in-beam test experiments were performed at GSI-Darmstadt using fragmented ^{12}C ion beam at 1.5A GeV delivered by the SIS accelerator. After a fragmentation target placed about 20 m up-stream from the test setup, the magnetic rigidity of the beam transport system was chosen for a selection of 1.5 GeV protons. Two overlapping scintillators (P_1, P_2) are used to focus the beam. They are followed by the spark detector placed between the two scintillators (M_1, M_2), which have a surface of 2.5 $\times$ 5 cm^2 and 2 cm thickness and are equipped with fast phototubes (Hamamatsu Hybrid H2431, rise time 0.7 ns). The electronics used for the 32 timing signals and the 16 amplitude signals are described in ref. [19].

Noble Gas	Resolution	Tails	Efficiency
Ar	100 ps	9 % (13 %)	96 %
Ne	90 ps	2 % (5 %)	85 %
Kr	130 ps	14 % (15 %)	92 %

Table 1: Efficiency, resolution and absolute tail for an Ar, Ne and Kr gas mixture.

Since the area covered by the scintillators is smaller than the spark counter and positioned well inside the edges of the active area, the ratio between the number of registered sparks with respect to the number of triggers delivers an accurate value for the spark counter efficiency. The ToF is defined as followed:

$$ToF = t_{pes} - \frac{1}{2}(t_{m1} + t_{m2})$$

where t_{pes} is the average of t_{left} and t_{right}, the times measured on both ends of the strip which has the highest amplitude. Due to a non gaussian time response shape of the ToF, an estimation of the tail proportion is introduced. The absolute tail is then defined as the proportion of events outside the window of $\pm$ 300 ps respect to the total number of event, while the relative tail is the proportion of events outside the gaussian respect to the total number of events.

In this section, we will briefly report about the mean results of the PesToF detector tests, more details could be found in ref. [19]. Different parameters were changed in order to optimize the detector response, as nature of the noble gas, gas pressure and so on.

Table 1 gives the resolution, the proportion of tails and the efficiency for an Argon, Neon and Krypton gas mixture. Due to its higher atomic number, a better time response for Argon gas mixture would have been expected. Indeed a better efficiency is achieved compared to Neon gas mixture (ϵ_{Ar} = 96 %, ϵ_{Ne} = 85 %). But the obtained resolution is much improved with this latter, this is to be related to a higher Townsend coefficient (inverse of the mean free path) and a higher drift velocity of the electron in the avalanche [17, 19]. This argument holds true as well for a krypton gas mixture.

The measurements were performed with a relatively poor electronic resolution and therefore the resolution was found to be around 100 ps. Measurements performed after with a 90 cm detector have given a excellent time response. The intrinsic time resolution was found to be lower than 60 ps and the proportion of absolute tails was less than 1.5 %. The time response function of the 90 cm counter is plotted in figure 5. The results were obtained with a Neon gas mixture flowing through the detector, this latter was tilted with an angle of 45^o respect to the perpendicular of the beam axis.

The resolution of the PesToF fulfilled the requirements of the FOPI upgrade project. Due to delay and technical problems with the manufacturing of the glass anode and also due to developments in the ToF techniques, a new type of detector has been considered GRPC for the ToF of FOPI. This alternative solution, as it shall be described later besides excellent timing response offers a number of advantages for the technical realization and the operation in a ToF system.

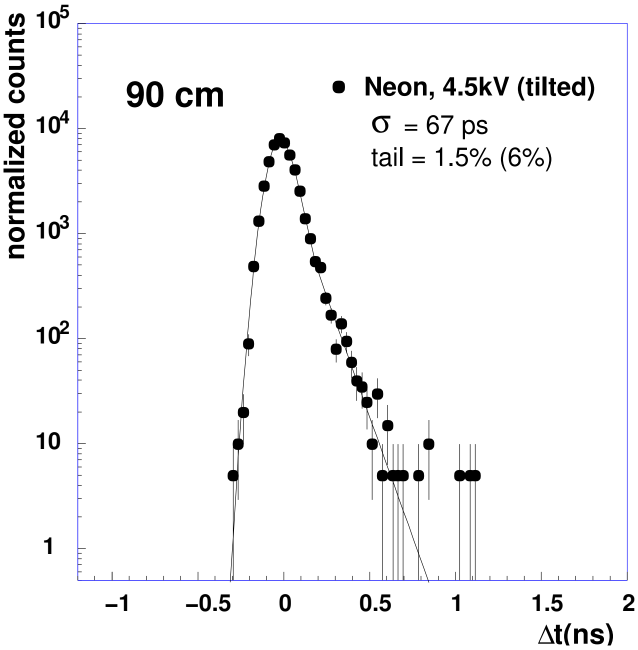

Figure 5: Time function response for a 90 cm PesToF counter.

6 Single cell Glass Resistive Plate Chamber

GRPC with internal floating glass and metal electrodes were used recently. In the framework of ALICE-ToF, a 3×3 cm^2 single cell GRPC was developed in a collaboration work of CERN and LIP Coimbra [11]. Encouraged by the excellent time response obtained by this single cell GRPC, the FOPI collaboration, in a joint effort with the LIP Coimbra, has started the development of GRPCs in view of the ToF upgrade. Several different prototypes of chambers were tested under beam. In this section, we will only report about the last developments and tests realized at the CERN-PS accelerator.

The chamber used in this beam test is schematically depicted in fig 6. A 5 cm diameter commercial (Athermal: $\rho \sim 10^{12}$ Ω·cm) welding glass with a thickness of

3 mm is glued onto a cylindrical printed board (PB). The 2 mm thick, polished aluminum electrode is glued on plastic-copper support. This plate is slightly smaller than the glass one, in order to reduce discharge to the PB and reduce the distortion of the electric field at the edge of the active area. The support is soldered on the PB. The mechanical precision of the gaps has been estimated to be less than 10 μm.

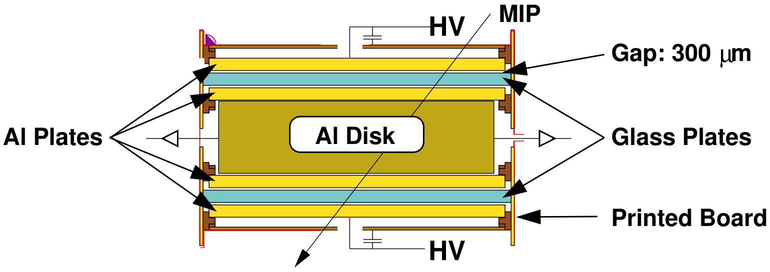

Figure 6: Schematic view of a single cell GRPC.

The readout of the GRPC is performed through an aluminum disk which is fixed on the electrode with a double face copper tape. The readout could then be placed on two diametral opposite sides of the disk. After an avalanche have occurred, an alteration of the electric field due to the reminiscence of the charge on the anode could happen. A voltage divider (2×136 MΩ) is used to set the glass anode at a given high voltage to ensure a stable electric field.

The cells were installed in a tight gas box that was kept under continuous flow of a gas mixture consisting of 85 % of freon ($C_2H_2F_4$), 10 % of sulphur hexafluoride (SF_6) and 5 % of isobutane (C_4H_{10}). Tests were performed at CERN-PS using a secondary beam (T9-10) at 3.5 and 7 GeV/c mostly charged pions. The scintillators (2×8 cm^2) are put in a cross position giving a 2×2 cm^2 trigger beam area in the overlapping region. The scintillators are readout on both side giving a independent timing respect to the position. Behind the chamber a scintillator (1.4×1.4 cm^2 area) and a veto paddle scintillator are installed. This leads to an area that triggers the data acquisition of about 3 cm^2 with a rate under 100 Hz/cm^2. The efficiency of the GRPC could be deduced in the same manner as for the PesToF detector. The signals out of the GRPC are amplified with a current sensitive pre-amplifier. The discriminater works in a leading edge mode and the signals are digitalized with a commercial TDC with a 50 ps bin. The electronics has been developed at LIP Coimbra and a resolution better than 25 ps has been measured [20]. In addition the signals are sent to a charge integrating ADC (time integration: 300 ps). This latter is used for correcting the time shift as function of the amplitude. Charge and time signals of the scintillators are readout with standard commercial TDC and ADC. The ToF is defined in the same manner as for the PesToF counter with the GRPC time signal T_{RPC} being the average value of the both output time signals.

The time response of the chamber was determinated when the trigger area ($\sim$ 3 cm^2) coincide with the center of the GRPC. The result for 6.3 kV applied high voltage is shown in fig. 7, the proportion of streamer events are less than 20 %. The obtained resolution is around 50 ps and the amount of tail has a value of $\sim$ 0.1 %.

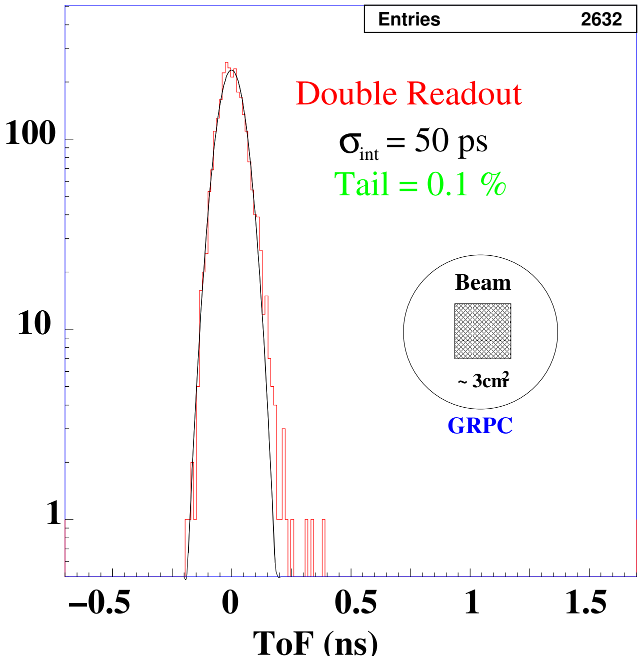

Figure 7: Time function response for a single cell GRPC.

In order to get information about possible edge effects, measurements were performed at different positions along the X-axis (along the readout line). The chamber was centered at position X = 0. Figure 8 presents the results for the charge, resolution and proportion of tails as a function of X-position for the single (open circle) and double (full circle) readout chamber. The charge decrease on the edge (X = ± 25 mm) about 20 %, related to loss of the influenced signal. No significant difference is seen between the single and double readout in terms of resolution. In addition, only a 10 ps deterioration in time resolution is observed when irradiating the edge of the chamber. One important feature of the double readout is a strong reduction of the amount of tail compared to the single readout. Measurements realized when the beam hits the most outer position of the chamber shows that the proportion of tail is less than 1 %. The time response function of the single cell GRPC is excellent and edge effects are weak.

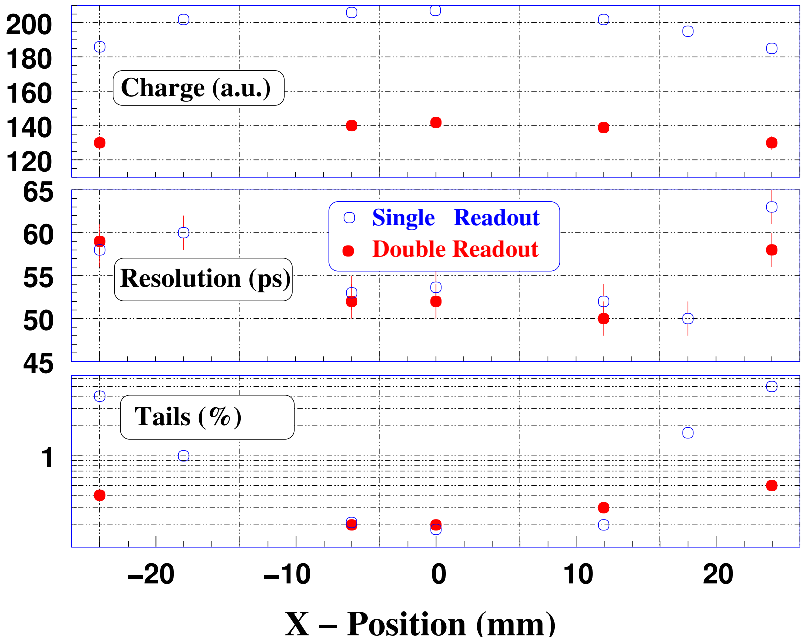

Figure 8: Time response of a single cell GRPC as a function of the X position.

7 Large area Glass Resistive Plate Chamber

Recently a large area GRPC using normal glass has been developed at LIP Coimbra, experiments as Harp [21] at CERN were strongly interested in such development for their ToF system. Since large area chamber reduce drastically the number of cells, this solution became also of interest for the FOPI collaboration. The chamber was built at LIP and was tested under beam condition at CERN. The chamber was built from 3 mm thick float-glass plates with an area of 160×12 cm^2 with a measured resistivity of 2×10^{12} Ω·cm. The stack of plates with attached copper foil electrode strips, 5 cm wide, (see fig. 9) was mounted on a supporting 1 cm thick acrylic plate and a controlled pressure was applied to the stack by means of regularly spaced spring-loaded plastic bars. Four gaps were defined by glass fibers of 300 μm placed between the glass plates, beneath the pressing bars [22].

As for the single cell chamber, the inner glass plates were kept at a given tension by a voltage divider. The same gas mixture as mentioned for the small GRPC was used. Measurements were performed using the same electronics provided by LIP Coimbra than for the small chamber .

Figure 10 shows the time response when irradiating the center of a strip, corrected for the walk of the time versus the charge. The obtained intrinsic resolution is around 60 ps with less than 1 % absolute tail and an efficiency

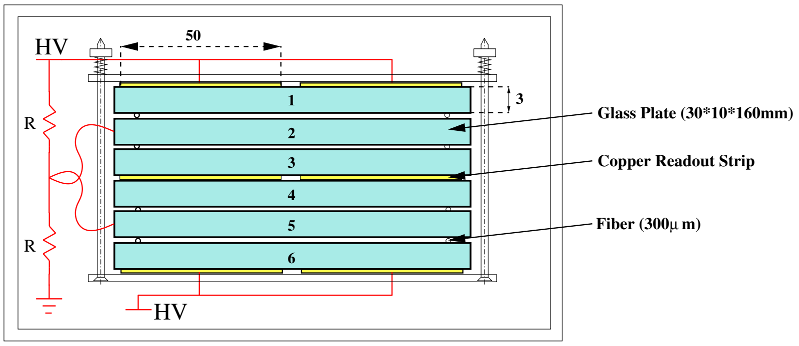

Figure 9: Schematic view of the large area GRPC. The GRPC is depicted in a front view. At the end of the strips, the signals are fed in the pre-amplifier.

higher than 97 %.

Scanning along the strip axis in step of 12 mm, shown a quite regular behavior of the efficiency, resolution and proportion of tails, for both strips. In average a efficiency greater than 97 % was achieved with an intrinsic resolution better than 65 ps and a fraction of tail less than 1.5 %.First measurements with the 5 cm wide strips indicate a level of 80 % cross-talk between strips, this do not affect the resolution but leads to a reduced double hit capability of multi-strip chambers.

Besides a high efficiency the GRPC gives an excellent time response, the resolution is better than 70 ps with a low proportion of absolute tails. These performances of the GRPC are not affected by the size of the chamber. This makes the application of the GRPC for a ToF system very flexible and convenient for any granularity. The simple construction with normal floating glass is an attractive feature of these chambers compared to PesToF counters. Another advantage of this techniques lies in the use of non-flammable gas at atmospheric pressure.

8 Possible designs for a GRPC array

For the purpose of the FOPI project, the new ToF system based on GRPC should cover at least the polar angle of $38^o < \theta < 65^o$ in a cylindrical geometry with a radius of one meter. We will discussed in this section two possible solutions based on single shielded GRPC. Cross-talk between neighboring pads or strips or reciprocal influence of electronic channels could be avoid in such a configuration.

A first solution is based on a single cell GRPC as described in section 6. In an overlapped configuration of two layers as shown in fig. 11a), the number of 5 cm cells is about 2500 distributed over 16 rings. For a central colliding Au + Au

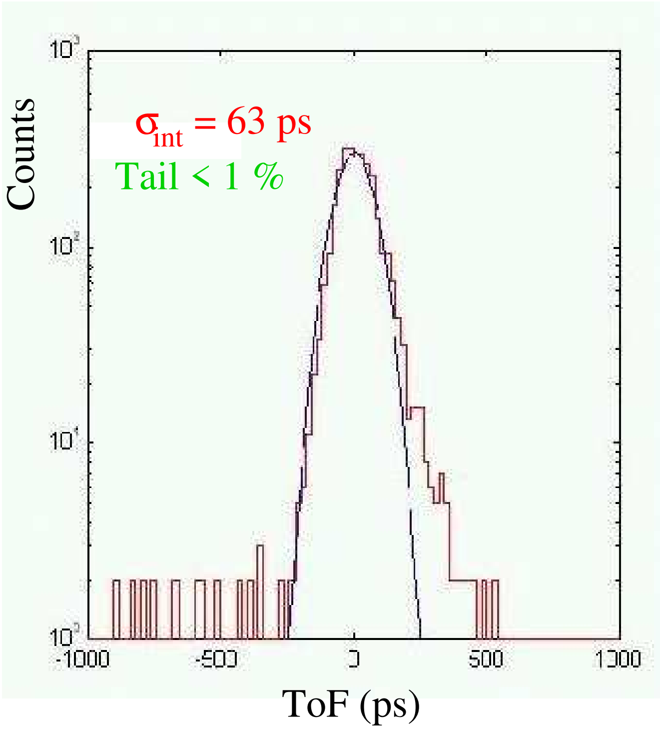

Figure 10: Time response function of the large area GRPC.

system at the highest SIS energy in the angular range ($38^o < \theta < 65^o$) of the new ToF of FOPI, the double hit probability can be estimated to be well below 1 %.

The second proposed solution is based on a striped GRPC as described in section 7, but with a single 2 cm wide readout strip. In a three layer configuration as depicted in fig. 11b) (upper part), the number of one meter long striped GRPC is 628. This leads to an estimated double hit probability of 4 %.

The hit position along the strip direction (X-axis) can be deduced from the time difference between the signal read out on both ends. In addition a y-position information (along the perpendicular direction of the strip) could be obtained by implemented narrow strips (see fig. 11b), lower part) on the outer high voltage electrodes and measuring the sharing of influenced charges. A timing GRPC with analog design for position measurement was successfully tested [23]. Besides a good position resolution, no deterioration of the time response was observed. Such position measurements are important for hit association between tracking chamber (CDC) and the ToF barrel. In addition it insures a efficient way of double hit recognition and rejection.

The important number of cells for the first solution provides a negligible double hit probability but leads to an increase of the cost related to electronic channels and demands more mechanical work. The second solution has half number

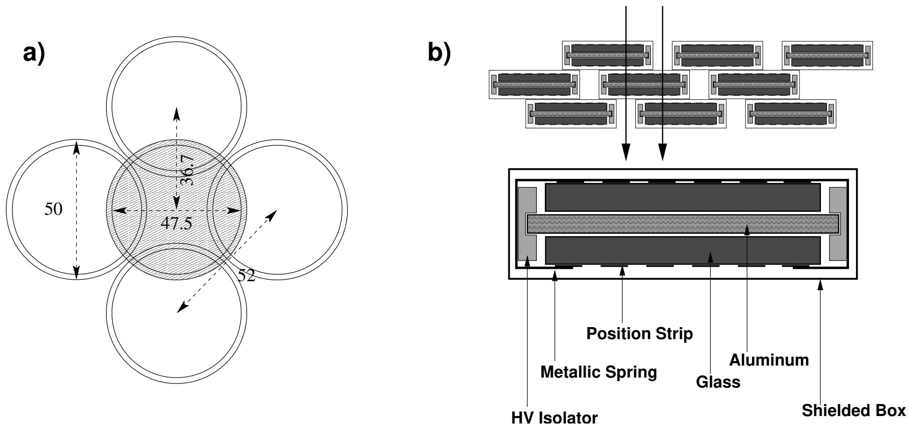

Figure 11: panel a): Schematic view of the a double layer configuration based on single cell GRPC. The second layer is symbolize by the dashed area. Panel b): Schematic view of a three layers configuration based on a single striped long GRPC. In the lower part is depicted the view of a single striped GRPC. The middle electrode is a bulk aluminum plate and the outer electrodes are normal floating glass. The strips on the high voltage electrodes are implemented for the position measurement.

of electronic channels (2×628), and has a 4 % double hit probability. Nevertheless the double hit could be rejected with the y-position measurement mentioned above. In order to reduce the mechanical effort a double gap configuration would be sufficient in view of the large overlap. The efficiency of a double gap GRPC was measured to be of 93 %.

In conclusion, the single striped solution presents several advantages an excellent time response, negligible tails, a high efficiency, good multi-hit capability and reasonable cost.

9 Conclusion

Data taken with the FOPI detector have evidenced an enhancement of the K^-/K^+ ratio at mid-rapidity and anti-flow for K^+ in central collisions, that could not be explained without introducing in medium effects. However, a complete measurement of the strangeness sector could not be achieved in the present status of the FOPI detector mainly due to the limitation of the ToF system. Two new prototypes of gas detector, PesToF and GRPC were tested. Both type of counters give a good time response in terms of resolution and tails and with high efficiency. For the practical realization, the timing GRPC offers a number of advantage which have been discussed here in some details. Based on those results, it has been shown that the most promising solution for FOPI-ToF system would be an array of shielded single strips counters.

10 Acknowledgements

The authors would like to thank the LIP-Coimbra team for their technical support and especially Paulo Fonte for his fruitful discussion and for all his support. We would like also to acknowledge Adriano Gobbi without whom the development of GRPC would not have been started in the FOPI collaboration.

References

[1] C.M. Ko, G.Q. Li, J. Phys. **G22** (1996) 1673
C.M. Ko, V. Koch, G. Li, Annu. Rev. Nucl. Part. Sci. **47** (1997) 1
and reference therein

[2] M. Menzel et al., Phys. Lett. **B495** (2000) 26

[3] Ph. Crochet et al., Phys. Rev. **B486** (2000) 2062

[4] K. Wiesniewski et al., Eur. Phys. J. **A9** (2001) 515

[5] http://www.star.bnl.gov/STAR/

[6] Technical Design Report: http://alice.web.cern.ch/Alice/TDR/

[7] Design Report CERN/AC/95-05(LHC) (1995)

[8] RHIC Design Manual:
http://www.rhichome.bnl.gov/NT-share/rhicdm/00_toc1i.htm

[9] V.V. Parkhomchuck, Yu.N.Pestov and N.V. Petrovykh, N.I.M. **A93** (1971) 269

[10] Yu.N.Pestov, Proceedings of . 26th Int. Winter Meeting on Nucl. Physics, Bormio (1998)

[11] P. Fonte et al., N.I.M. **A449** (2000) 295

[12] A. Gobbi et al., N.I.M. **A324** (1993) 156

[13] G.Q. Li and G.E. Brown Phys. Rev. **C58** (1998) 1698

[14] W. Cassing and E.L. Bratkovskaya, Phys. Rep. **308** (1999) 65

[15] Q. Pan and P. Danielewicz, Phys. Rev. Lett. **70** (1993) 2062

[16] R. Kutsche, thesis GSI-2000-05 (2000)

[17] A. Mangiarotti et al., submitted to N.I.M.A

[18] W.B.Atwood, et al., N.I.M. **A206** (1983)

[19] A. Devismes et al., accepted for publication in N.I.M.A

[20] A. Blanco et al., submitted to N.I.M.A

[21] Proposal CERN-SPSC/99-35

[22] P. Fonte et al., submitted to N.I.M.A

[23] P. Fonte et al., proceeding of the 9^{th} Vienna Conference on Instrumentation, Vienna / Austria, February 19 - 23, 2001